



Pergamon

Bioorganic & Medicinal Chemistry 10 (2002) 3627–3636

BIOORGANIC &  
MEDICINAL  
CHEMISTRY

## Phospholipid-Bound Molecular Rotors: Synthesis and Characterization

Mark A. Haidekker,<sup>a</sup> Thomas Brady,<sup>b</sup> Ke Wen,<sup>b</sup> Cliff Okada,<sup>a</sup> Hazel Y. Stevens,<sup>a</sup>  
Jeniffer M. Snell,<sup>a</sup> John A. Frangos<sup>a</sup> and Emmanuel A. Theodorakis<sup>b,\*</sup>

<sup>a</sup>Department of Bioengineering, University of California, San Diego, La Jolla, CA 92093-0412, USA

<sup>b</sup>Department of Chemistry and Biochemistry, University of California, San Diego, La Jolla, CA 92093-0358, USA

Received 28 March 2002; accepted 26 April 2002

**Abstract**—Molecular rotors are fluorescent molecules with a viscosity-sensitive quantum yield that are often used to measure viscosity changes in cell membranes and liposomes. However, commercially available molecular rotors, such as DCVJ (**1**) do not localize in cell membranes but rapidly migrate into the cytoplasm leading to unreliable measurements of cell membrane viscosity. To overcome this problem, we synthesized molecular rotors covalently attached to a phospholipid scaffold. Attaching the rotor group to the hydrophobic end of phosphatidylcholine (PC) did not affect the rotor's viscosity sensitivity and allowed adequate integration into artificial bilayers as well as complete localization in the plasma membrane of an endothelial cell line. Moreover, these new rotors enabled the monitoring of phospholipid transition temperature. However, attachment of the rotor groups to the hydrophilic head of the phospholipid led to a partial loss of viscosity sensitivity. The improved sensitivity and exclusive localization in the cell plasma membrane exhibited by the phospholipid-bound molecular rotors suggest that these probes can be used for the study of membrane microviscosity.

© 2002 Elsevier Science Ltd. All rights reserved.

### Introduction

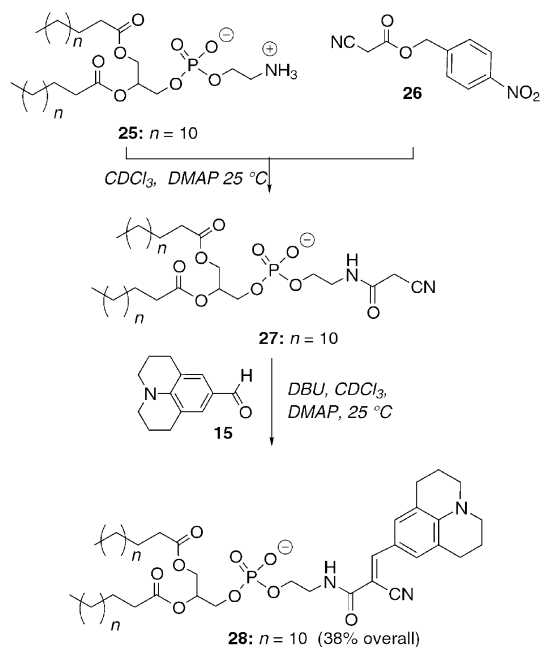
Cellular membranes are remarkable molecular assemblies, composed mainly of phospholipids and proteins, that play a central role in both the structure and the function of cells.<sup>1</sup> Perhaps the best way to visualize a membrane is to consider the 'fluid mosaic model' first described by Singer and Nicolson.<sup>2</sup> In this model the membrane is pictured as a fluid-like phospholipid bilayer, into which are embedded proteins. An important element of this model is the recognition that the membrane is a dynamic structure and its fluidity influences the structure and position of proteins, thereby affecting the physiological function of cells. Consequently, changes in membrane fluidity have been linked with alterations in physiological processes, such as carrier-mediated transport, activities of membrane-bound enzymes and receptor binding which, in turn, are associated with aging and disease pathogenesis. The importance of membrane viscosity in cellular biology and physiology led to the development of several fluorescence-

based methods<sup>3</sup> that have been used to assess the local viscosity of both cell membranes and model membranes (such as liposomes and vesicles). Among them are included: fluorescence recovery after photobleaching (FRAP),<sup>4</sup> fluorescence anisotropy (or fluorescence polarization)<sup>5</sup> and the use of environment-sensitive fluorescent probes.<sup>6</sup> In the latter category are included compounds such as 9-(dicyanovinyl)-julolidine (DCVJ, **1**) (Fig. 1) with a viscosity-dependent fluorescence quantum yield.

The intriguing fluorescent properties of DCVJ (**1**) rest upon its ability to lose the excited state either by radiation or by intramolecular rotation, the ratio of which depends on the free-volume of the environment.<sup>7</sup> This ability has defined a new class of molecules commonly referred to as *molecular rotor*,<sup>8</sup> that have been used as membrane viscosity sensors in both chemical and biological processes. While DCVJ allows the probing of the cell membrane viscosity it also localizes in the cell interior, showing a particular affinity to tubulin structures.<sup>9</sup> Cognizant of this limitation, we developed recently a more lipophilic analogue of DCVJ, referred to as FCVJ (**2**), in which a farnesyl side chain was attached to the viscosity-sensitive julolidine fragment.<sup>10</sup>

\*Corresponding author. Tel.: +1-858-822-0456; fax: +1-858-822-0386; e-mail: etheodor@ucsd.edu





**Scheme 2.** Synthesis of probe **28** in which the rotor is attached at the hydrophilic end of a phospholipid.

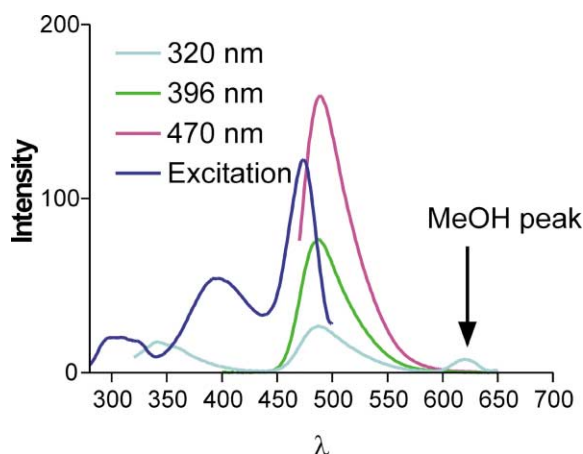


**Figure 2.** Excitation and emission spectra of the phospholipid-bound molecular rotor **22**. Three excitation maxima at 320, 396, and 470 nm have been observed. All three excitation wavelengths lead to an emission maximum at 490 nm. The small peak at 620 nm, which is only visible for 320 nm excitation, is caused by the solvent, methanol. Compounds **23**, **24**, and **28** show very similar spectra.

490 nm. The emission intensity is highest for excitation at 470 nm. Fig. 2 shows the excitation spectrum as well as the emission spectra for all three excitation maxima for compound **22**. Similar spectra were obtained for compounds **23**, **24**, and **28**. All subsequent experiments were performed at  $\lambda_{ex} = 470$  nm and  $\lambda_{em} = 490$  nm.

To verify the rotor properties of the above compounds we examined the relationship between their quantum yield of fluorescence emission and solvent viscosity. This was accomplished using mixtures of ethylene glycol and glycerol as solvents. Compounds **22**, **23**, and **24** (but not

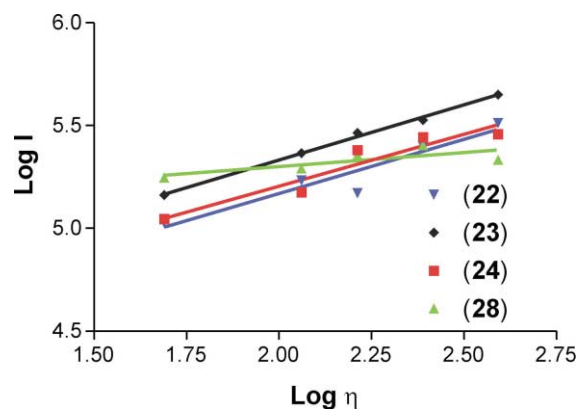


**Figure 3.** Assessment of the rotor behavior of compounds **22**, **23**, **24**, and **28**. All molecules except compound **28** show a power-law increase of the measured intensity ( $\lambda_{ex} = 470$  nm,  $\lambda_{em} = 490$  nm) with the viscosity of the solvent. With the exception of compound **28**, the slopes of the fitted lines were found to be in the range 0.48–0.53, which is similar to DCVJ (slope of 0.6).

compound **28**) showed the profile of a fluorescent rotor, characterized by an increase in the intensity of fluorescence emission by increasing the viscosity of the solvent (Fig. 3).<sup>12</sup> The results are in agreement with a power law relationship of quantum yield ( $\Phi$ ) and viscosity ( $\eta$ ), as indicated by the Förster–Hoffmann equation (eq 1).<sup>13</sup>

$$\text{Log } \Phi = C + x \cdot \text{log } \eta \quad (1)$$

The constant  $x$  in eq 1 is a dye-dependent constant and was found to be  $0.52 \pm 0.01$  for **22**,  $0.53 \pm 0.02$  for **23**,  $0.48 \pm 0.029$  for **24**, and  $0.21 \pm 0.12$  for **28**; data given as mean  $\pm$  standard deviation from three independent experiments. This indicates that probes **22**, **23**, and **24** (but not **28**) exhibit a rotor behavior similar to DCVJ (**1**), where the constant  $x$  is known to be 0.6.<sup>10</sup>

#### Integration of phospholipid-bound molecular rotors in artificial membranes

To examine if our designed probes retain their rotor properties when embedded in cellular membranes or model membranes, we studied their fluorescent emission as a function of temperature in liposome bilayers. It is known that DCVJ (**1**), when integrated into an artificial bilayer consisting of dimyristoyl-phosphatidylcholine (DMPC), shows an emission intensity which is inversely related to the temperature.<sup>14</sup> This may be explained by considering that increase of temperature can lead to both an increase of intramolecular rotation of the rotor and a decrease of phospholipid viscosity. Similar effects were observed for compounds **22**, **23**, and **24**. Above the transition temperature of DMPC at 23 °C, the rate of decrease of the temperature-dependent intensity is markedly reduced (Fig. 4, top panel). Between 23 and 25 °C we observed a transition with a steeper gradient:  $-0.17\%$  as opposed to  $13\%$ , observed below 23 °C and  $-4\%$ , observed above 25 °C (slopes have been normalized to the absolute intensity at 40 °C). When using **23**,

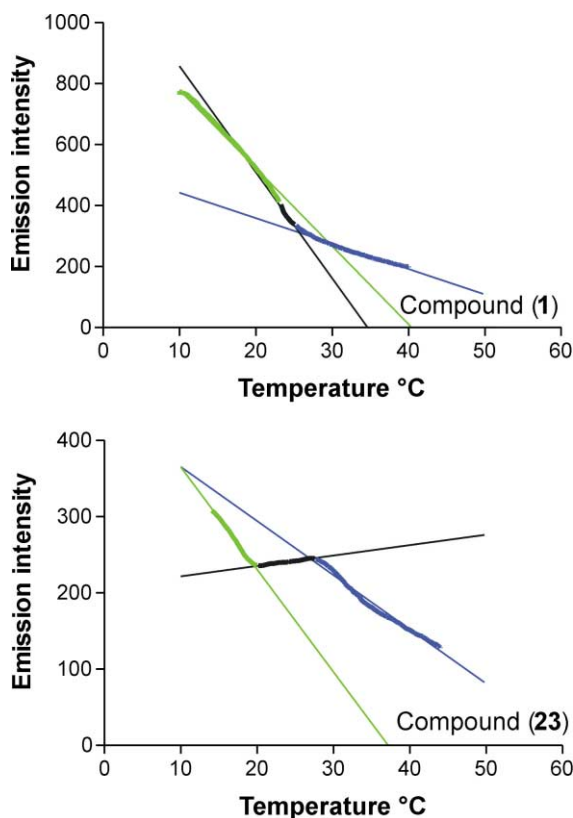


**Figure 4.** Decrease of emission intensity of DCVJ (**1**) and the phospholipid-bound rotor **23** incorporated in phosphatidylcholine bilayers. The transition temperature of pure phosphatidylcholine is 23 °C. While at this temperature **1** merely changes its slope, compound **23** shows a distinct inversion of the slope, clearly marking the transition from the gel- to the liquid-crystal phase. The thin lines indicate regression lines fitted into the data within the three distinctly different phases: Gel (green), transition (black) and liquid-crystal (blue).

an inversion of the slope becomes visible between 23 and 27 °C. Normalized to the intensity at 40 °C, the slopes were  $-9\%$  below 23 °C,  $+1\%$  between 23 and 27 °C, and  $-5\%$  above 27 °C. Above 27 °C, the normalized slopes of compounds **1** and **23** are similar. Compound **28** does not show this inverted slope. Below 23 °C, a slope of  $-10\%$  was found, between 23 and 27 °C  $-12\%$ , and above 27 °C  $-6\%$ .

#### Localization of the probes in cultured cells

To determine the extent of cell membrane localization of our synthesized probes we compared their staining to that of commercially available probe DiI-C<sub>18</sub>, a dye known to localize exclusively in plasma membrane.<sup>15</sup> Cells of the endothelial cell line, ECV-304, plated onto coverslips, were dual-labeled with DiI-C<sub>18</sub> and one of the compounds **22**, **23**, **24**, or **28**, and the staining was examined using an epifluorescent microscope. In all four cases, a clear co-localization of DiI with the phospholipid-bound rotor could be seen (Fig. 5). A darker spot indicating nuclear or nucleolar staining, which would indicate internalization, was not observed. This indicates that the phospholipid-bound molecular rotors localize exclusively in the plasma membrane. It is worth noting that dye **22** exhibits some cytotoxicity, as sug-

gested by the cell detachment (see Fig. 5, top row). Nonetheless, this detachment is not observed with compounds **23**, **24**, and **28**, indicating that these probes can be used in cell-based studies.

#### Discussion

Driven by the need to understand cell membrane function, various fluorescent-based methods to measure cell membrane viscosity have been developed. These methods include: FRAP (fluorescence recovery after photobleaching),<sup>5</sup> and fluorescence anisotropy (or fluorescence polarization).<sup>6</sup> Although both methods allow a direct, quantitative measurement of local viscosity they have, nonetheless, distinct disadvantages. FRAP requires a relatively long time for the measurement to allow sufficient fluorescence recovery, limiting both the spatial and temporal resolution.<sup>16</sup> Also, the photobleaching laser pulse introduces power densities up to 1 MW/cm<sup>2</sup> to the membrane, leading to generation of free radicals by photolysis and to local heating which in turn damages the surrounding proteins and decreases the apparent viscosity due to protein cross-linking.<sup>18</sup> On the other hand, measurement of fluorescence anisotropy is mostly limited by the need for polarization filters, which absorb a large amount of the emitted light, thereby reducing sensitivity.<sup>17</sup> Due to photobleaching effects, excitation light cannot be increased to fully compensate for polarizer absorption. In addition, the mathematical treatment of anisotropy results, when used to compute viscosity, has been subject to controversy.<sup>18,19</sup> A third fluorescence-based method used to assess membrane viscosity relies on the use of environment-sensitive fluorescent probes. In this category are included fluorescent molecules, such as DCVJ (**1**) that exhibit a viscosity-dependent fluorescence quantum yield. These compounds, often referred to as ‘molecular rotors’, are particularly attractive to use since by simply measuring their fluorescence intensity we can obtain information on viscosity changes. Nonetheless, the major disadvantage of currently available molecular rotors is their affinity to cellular organelles other than the plasma membrane. For example, a strong affinity of DCVJ (**1**) for tubulin leads to areas of strong intracellular fluorescence, which reduce measurement sensitivity through inactive background fluorescence.

To improve the membrane localization profile of such rotors we sought to attach them to a phospholipid backbone using a polymethylene linker. Two strategies were developed allowing attachment of the julolidine scaffold at either the non-polar or the polar end of a phospholipid (compounds **22**, **23**, **24**, and compound **28**, respectively).

The molecular rotors synthesized in this study exhibit a complex fluorescence pattern with triple excitation maxima, but a single emission maximum. The most widespread molecular rotor, DCVJ (**1**), shows only two single excitation maxima.<sup>19</sup> The emission intensity of our synthesized rotors depends on the viscosity of the solvent, in a manner similar to DCVJ. Examination of compounds

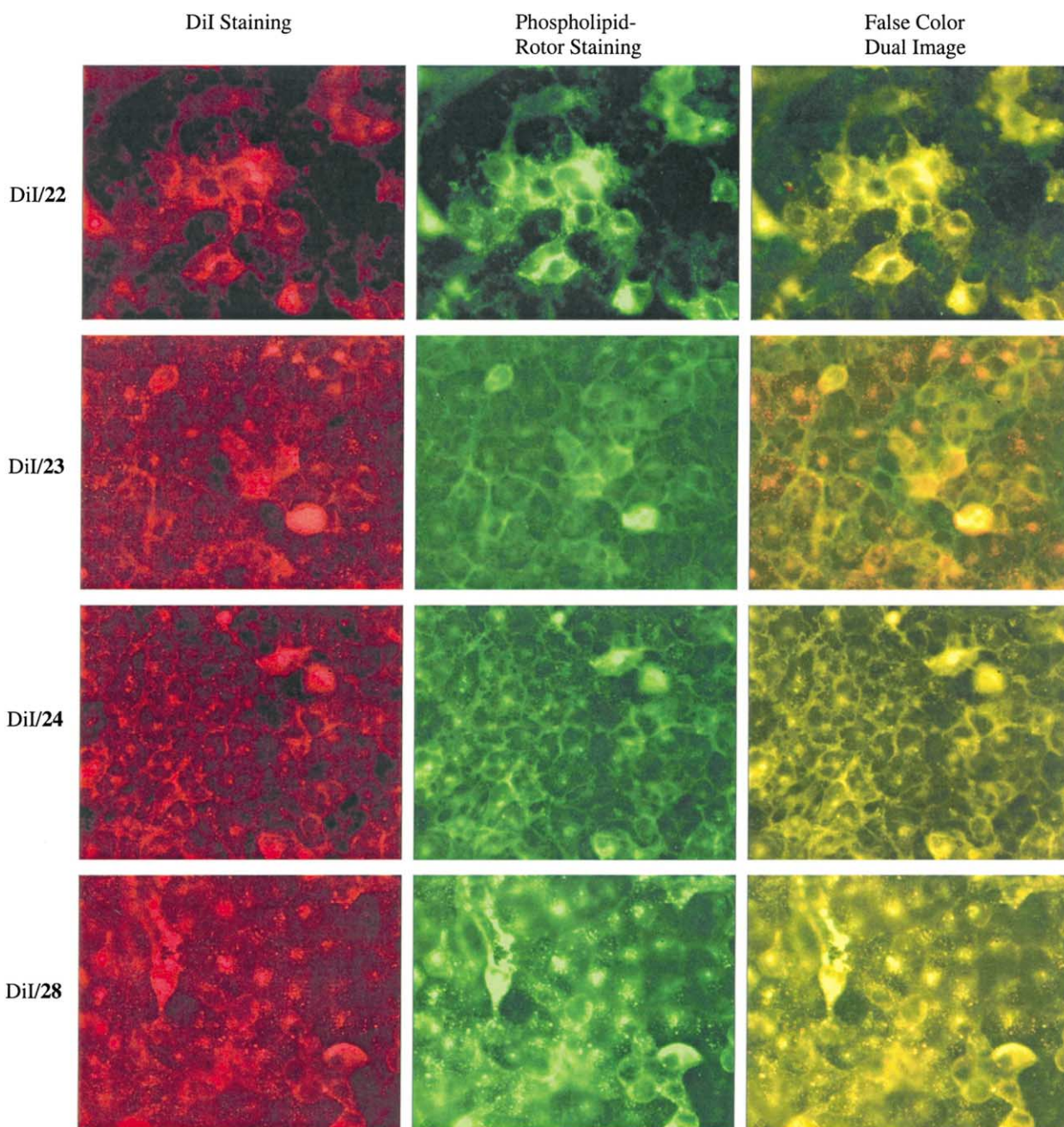


**Figure 5.** Dual stained cells of the ECV-304 line. The first column shows DiI-staining, while the second column shows fluorescence generated by the probes **22** (top row), **23** (second row), **24** (third row), and **28** (bottom row). The false-color image in the third column shows DiI-staining in red and the staining with the phospholipid-bound rotor in green. Yellow hues appear where both dyes are present. DiI and all phospholipid-bound probes show similar staining patterns indicating that these dyes localize in the membrane. Cell detachment caused by **22** can be seen (top row) but is not observed with the other probes.

**22**, **23**, and **24** indicated that they have a slightly lower slope (ca. 0.5) than DCVJ and FCVJ (ca. 0.6).<sup>10</sup> Nonetheless, this decrease of slope does not translate to a significant loss of viscosity sensitivity, particularly when the probe is localized in cell membranes. Moreover, the viscosity sensitivity of compounds **22**, **23** and **24** suggests that the rotor–environment interaction is not affected if the rotor is attached to the hydrophobic end of the phospholipid. However, compound **28** (having the rotor attached at the polar end of a phospholipid) was found to have a significantly reduced exponent  $x$  in the Förster–Hoffmann relationship (eq 1). This suggests that

interactions exist within the phospholipid-dye molecule that inhibit free interaction with the environment, leading to reduced viscosity sensitivity.

It has been observed that molecular rotors can be used to monitor the phase transition of phospholipids.<sup>16</sup> We used this property to establish the behavior of phospholipid-bound rotors in phospholipid bilayers. As expected, we found changes of the gradient (intensity change over temperature change) at the transition temperature of phosphatidylcholine liposomes using DCVJ (**1**) as a probe.<sup>16</sup> The transition phase is even more

clearly marked by a temporary increase in intensity when using phospholipid-bound rotor **23** (see Fig. 4, bottom panel). The behavior of phospholipid bilayers at the transition temperature is not fully understood. Studies suggest that in the liquid-crystal state close to the transition temperature, local gel-phase domains exist, and furthermore, surface viscosity increases significantly.<sup>20</sup> This would be consistent with the increase in intensity observed with molecular rotors bound to phospholipids (such as **23**). It is worth noting that this increase is not observed with DCVJ. This, in turn, suggests that the synthesized phospholipid-bound rotors reflect more accurately changes in phospholipid transition phase of liposomes and related membrane models.

When the rotor group is attached to the hydrophilic end (see probe **28**), the gradient inversion observed with **22**, **23**, and **24** is not visible. Failure of compound **28** to exhibit viscosity sensitivity may be due to the loss of zwitterionic character of the phospholipids structure and the presence of a phosphate anion close to the julolidine part. The difference between the slopes in the gel- and the liquid-crystal phase is even lower than with DCVJ, which is consistent with the diminished viscosity sensitivity stated earlier. We therefore consider compound **28** not to be useful as a membrane probe.

The excellent localization of all synthesized phospholipid bound rotors in cell plasma membrane, is illustrated in Figure 5. The co-localization study with the known membrane dye DiI-C<sub>18</sub> clearly shows similar staining patterns for both dyes. A darker area at the location of the cell nucleus, as observed with DCVJ and—to a lesser extent—the farnesyl derivative FCVJ (**2**) was not observed with **22**, **23**, **24**, or **28**. These results suggest that all phospholipid-bound rotors remain attached to the plasma membrane with negligible transfer into the interior of the cell. However, it was also observed that under the experimental conditions of this study, compound **22** leads to cell detachment, an indication of cytotoxicity. This effect may be due to the introduction of a short (C-8) phosphatidylcholine conjugate that interferes with the structure of the cell membrane. Such cell detachment was not observed with the longer phospholipid conjugates **23** and **24**. Based on the false-color images (Fig. 5) we can conclude that phospholipid-bound rotor **24** shows identical localization profile with DiI-C<sub>18</sub>, rendering it a probe of choice for studies of cell membrane viscosity.

### Conclusion

To improve the membrane localization of DCVJ and related fluorescent rotors, we attached the julolidine fragment to either end of a phospholipid structure. All compounds exhibited the desired membrane localization profile, which was comparable to that of the commonly used membrane dye DiI. Only compounds in which the rotor was attached to the non-polar end of the phospholipid (such as **22**, **23**, and **24**) displayed the characteristic property of a fluorescent rotor, which is the viscosity dependent fluorescence emission quantum yield. Among

these, rotor **24** exhibited an identical localization profile with DiI. Compound **28**, in which the rotor was attached to the polar end of the phospholipid was devoid of such properties.

## Materials and Methods

### General techniques

Lysophospholipids **20**, **21**, and **25** were purchased from Avanti, Polar Lipids, Inc., AL, USA and used without any additional purification. All reagents were commercially obtained (Aldrich, Acros) at highest commercial quality and used without further purification except where noted. Air- and moisture-sensitive liquids and solutions were transferred via syringe or stainless steel cannula. Organic solutions were concentrated by rotary evaporation below 45 °C at about 20 mmHg. All non-aqueous reactions were carried out using flame-dried glassware, under an argon atmosphere in dry, freshly distilled solvents under anhydrous conditions, unless otherwise noted. Tetrahydrofuran (THF) and diethyl ether (Et<sub>2</sub>O) were distilled from sodium/benzophenone; dichloromethane (CH<sub>2</sub>Cl<sub>2</sub>) and toluene from calcium hydride; and benzene from potassium. *N,N*-Diisopropylethylamine, diisopropylamine, pyridine, triethylamine and boron trifluoride etherate were distilled from calcium hydride prior to use. Yields refer to chromatographically and spectroscopically (<sup>1</sup>H NMR) homogeneous materials, unless otherwise stated. Reactions were monitored by thin-layer chromatography carried out on 0.25 mm E. Merck silica gel plates (60F-254) using UV light as visualizing agent and 7% ethanolic phosphomolybdic acid, or *p*-anisaldehyde solution and heat as developing agents. E. Merck silica gel (60, particle size 0.040–0.063 mm) was used for flash chromatography. Preparative thin-layer chromatography separations were carried out on 0.25 or 0.50 mm E. Merck silica gel plates (60F-254). NMR spectra were recorded on Varian Mercury 300, 400 and/or Unity 500 MHz instruments and calibrated using residual undeuterated solvent as an internal reference. The following abbreviations were used to explain the multiplicities: s=singlet; d=doublet, t=triplet, q=quartet, m=multiplet, b=broad. IR spectra were recorded on a Nicolet 320 Avatar FT-IR spectrometer and values are reported in cm<sup>-1</sup> units. High resolution mass spectra (HRMS) were recorded on a VG 7070 HS mass spectrometer under chemical ionization (CI) conditions or on a VG ZAB-ZSE mass spectrometer under fast atom bombardment (FAB) conditions.

**Ester 6.** To a solution of 5.7 g of 4-methoxy benzyl alcohol (**5**) (28.9 mmol) and 3.5 g of DMAP (29 mmol) in 50 mL of dichloromethane under argon at 0 °C were added dropwise 5.7 g of 6-bromo hexanoyl chloride (27 mmol). The reaction mixture was then allowed to warm up to 25 °C, where it was stirred for 2 h. The DMAP-HCl salt was filtered off by gravity filtration and the mixture was concentrated under reduced pressure. The resulting oil was filtered through a short silica plug with hexane. The solvent was then removed to give 7.5 g of benzyl ester **6** (23.8 mmol, 82%), which was used in the

next reaction without further purification. **6**: colorless liquid; IR (film)  $\nu_{\max}$  1732;  $^1\text{H}$  NMR (400 MHz,  $\text{CDCl}_3$ )  $\delta$  7.39 (2H, d,  $J=6.4$ ), 6.89 (2H, d,  $J=6.4$ ), 5.05 (2H, s), 3.81 (3H, s), 3.38 (2H, t,  $J=6.8$ ), 2.34 (2H, t,  $J=7.2$ ), 1.85 (2H, m), 1.65 (2H, m), 1.45 (2H, m);  $^{13}\text{C}$  NMR (100 MHz,  $\text{CDCl}_3$ )  $\delta$  173.1, 159.3, 130.0, 127.9, 113.8, 66.0, 55.3, 34.1, 33.6, 32.4, 27.7, 24.1; HRMS, calcd for  $\text{C}_{14}\text{H}_{19}\text{BrO}_3$  ( $\text{M} + \text{Cs}^+$ ) 446.9568, found 446.9572.

**Ester 7**. Preparation of this compound was accomplished in 61% yield following the procedure described above for the synthesis of ester **6**. **7**: white solid; IR (film)  $\nu_{\max}$  1733;  $^1\text{H}$  NMR (400 MHz,  $\text{CDCl}_3$ )  $\delta$  7.30 (2H, d,  $J=8.8$ ), 6.90 (2H, d,  $J=8.8$ ), 5.05 (2H, s), 3.81 (3H, s), 3.42 (2H, t,  $J=6.8$ ), 2.34 (2H, t,  $J=8$ ), 1.85 (2H, m), 1.62 (2H, m), 1.27 (10H, s);  $^{13}\text{C}$  NMR (100 MHz,  $\text{CDCl}_3$ )  $\delta$  173.7, 159.4, 129.9, 128.1, 113.8, 113.8, 65.8, 55.2, 34.3, 34.0, 32.8, 29.3, 29.3, 29.1, 29.0, 28.7, 28.1, 24.9; HRMS, calcd for  $\text{C}_{19}\text{H}_{29}\text{BrO}_3$  ( $\text{M} + \text{Cs}^+$ ) 517.0351, found 517.0372.

**Azide 8**. A solution of 7.4 g of ester **6** (23.5 mol) and 1.7 g of sodium azide (26 mmol) in DMF (50 mL) was stirred at 25 °C for 12 h. The reaction mixture was diluted with water (200 mL) and extracted with ether (3×100 mL). The solvent was removed under reduced pressure and the resulting oil was chromatographed (silica, 10–30% ether in hexanes) to yield 6.1 g of compound **8** (22 mmol, 94%). **8**: colorless liquid; IR (film)  $\nu_{\max}$  2095, 1732;  $^1\text{H}$  NMR (400 MHz,  $\text{CDCl}_3$ )  $\delta$  7.29 (2H, d,  $J=6.4$ ), 6.89 (2H, d,  $J=6.4$ ), 5.05 (2H, s), 3.80 (3H, s), 3.25 (2H, t,  $J=6.8$ ), 2.34 (2H, t,  $J=7.2$ ), 1.68–1.54 (4H, m), 1.40 (2H, m);  $^{13}\text{C}$  NMR (100 MHz  $\text{CDCl}_3$ )  $\delta$  173.3, 159.6, 130.0, 128.1, 113.9, 66.0, 55.2, 51.2, 34.0, 28.5, 26.1, 24.3; HRMS, calcd for  $\text{C}_{14}\text{H}_{19}\text{N}_3\text{O}_3$  ( $\text{M} + \text{Cs}^+$ ) 410.0477, found 410.0491.

**Azide 9**. Preparation of this compound was accomplished in 92% yield following the procedure described above for the synthesis of azide **8**. **9**: colorless liquid; IR (film)  $\nu_{\max}$  2095, 1732;  $^1\text{H}$  NMR (400 MHz,  $\text{CDCl}_3$ )  $\delta$  7.28 (2H, d,  $J=8.8$ ), 6.88 (2H, d,  $J=8.8$ ), 5.03 (2H, s), 3.79 (3H, s), 3.23 (2H, t,  $J=7.2$ ), 2.30 (2H, t,  $J=7.6$ ), 1.59 (4H, m), 1.25 (12H, s);  $^{13}\text{C}$  NMR (100 MHz,  $\text{CDCl}_3$ )  $\delta$  173.3, 159.3, 129.7, 128.0, 113.6, 65.6, 54.9, 51.2, 34.1, 29.2, 29.1, 29.0, 28.9, 28.9, 28.6, 26.5, 24.7; HRMS, calcd for  $\text{C}_{19}\text{H}_{29}\text{N}_3\text{O}_3$  ( $\text{M} + \text{Cs}^+$ ) 480.1260, found 480.1272.

**Amino ester 10**. To a solution of 3.0 g of azide **8** (9.4 mmol) in THF (50 mL) were added 2.62 g of triphenylphosphine (10 mmol) and 1 mL of  $\text{H}_2\text{O}$ . After stirring at 25 °C for 12 h the reaction mixture was concentrated under reduced pressure and the remaining residue was dissolved in 75 mL of dichloromethane and washed with aqueous saturated sodium carbonate (2×50 mL). The organic layer was collected, dried over  $\text{MgSO}_4$  and concentrated. The residue was filtered through a short plug of silica (0–5% methanol in dichloromethane) to yield 2.1 g of the amino ester **10** (8.3 mmol, 88%) which was taken directly to the next step as it was prone to decomposition. **10**:  $^1\text{H}$  NMR (400 MHz,  $\text{CDCl}_3$ )  $\delta$  7.23 (2H, d,  $J=6.4$ ), 6.81 (2H, d,  $J=6.4$ ), 4.98 (2H, s), 3.74

(3H, s), 2.59 (2H, t,  $J=6.8$ ), 2.27 (2H, t,  $J=7.2$ ), 1.60–1.54 (4H, m), 1.40–1.36 (2H, m), 1.29–1.25 (2H, m);  $^{13}\text{C}$  NMR (400 MHz,  $\text{CDCl}_3$ )  $\delta$  173.5, 159.5, 132.0, 129.9, 128.5, 113.8, 65.8, 55.1, 41.7, 34.1, 26.3, 24.7; HRMS, calcd for  $\text{C}_{14}\text{H}_{21}\text{NO}_3$  ( $\text{M} + \text{H}^+$ ) 252.1594, found 252.1595.

**Amino ester 11**. Preparation of this compound was accomplished in 91% yield following the procedure described above for the synthesis of amino ester **10**. **11**: white solid;  $^1\text{H}$  NMR (400 MHz,  $\text{CDCl}_3$ )  $\delta$  7.30 (2H, d,  $J=6.8$ ), 6.89 (2H, d,  $J=6.8$ ), 5.04 (2H, s), 3.81 (3H, s), 2.69 (2H, t,  $J=6.8$ ), 2.33 (2H, t,  $J=7.6$ ), 1.60 (2H, m), 1.42 (2H, m), 1.27 (12H, s), 1.13 (2H, s);  $^{13}\text{C}$  NMR (100 MHz,  $\text{CDCl}_3$ )  $\delta$  173.6, 159.4, 129.9, 128.1, 113.8, 113.7, 65.8, 55.2, 41.0, 34.3, 30.7, 29.6, 29.4, 29.3, 29.1, 26.8, 24.9; HRMS, calcd for  $\text{C}_{19}\text{H}_{31}\text{NO}_3$  ( $\text{M} + \text{H}^+$ ) 322.2382, found 322.2390.

**Cyano ester 13**. To a solution of 2 g of amine **9** (8 mmol) and 0.68 g of cyano acetic acid (**12**) (8 mmol) in 15 mL of dichloromethane at 0 °C under argon was added dropwise a solution of 1.6 g DCC (8 mmol) in 5 mL of dichloromethane. When the addition was complete the ice bath was removed and the reaction was stirred at 25 °C for 3 h. 20 mL of hexane was then added to the reaction mixture and the DCU side-product was filtered off. The reaction mixture was concentrated under reduced pressure and the residue chromatographed (silica, 0–10% methanol in dichloromethane) to yield 1.3 g of compound **13** (4.1 mmol, 41%). **13**: colorless oil; IR (film)  $\nu_{\max}$  2305, 1725;  $^1\text{H}$  NMR (400 MHz,  $\text{CDCl}_3$ )  $\delta$  7.29 (2H, d,  $J=8.4$ ), 6.89 (2H, d,  $J=8.4$ ), 6.29 (1H, bs), 5.05 (2H, s), 3.81 (3H, s), 3.35 (2H, s), 3.28 (2H, q,  $J=7.2$ ), 2.34 (2H, t,  $J=7.6$ ), 1.65 (2H, m,  $J=8.0$ ), 1.54 (2H, m,  $J=7.2$ ), 1.34 (2H, m,  $J=7.2$ );  $^{13}\text{C}$  NMR (100 MHz,  $\text{CDCl}_3$ ) 173.2, 160.6, 159.4, 129.9, 127.9, 114.7, 114.4, 66.1, 55.3, 40.1, 34.0, 28.8, 26.2, 25.9, 24.3; HRMS, calcd for  $\text{C}_{17}\text{H}_{22}\text{N}_2\text{O}_4$  ( $\text{M} + \text{Cs}^+$ ) 451.0630, found 451.0619.

**Cyano ester 14**. Preparation of this compound was accomplished in 47% yield following the procedure described above for the synthesis of compound **13**. **14**: white solid; IR (film)  $\nu_{\max}$  2307, 1724;  $^1\text{H}$  NMR (400 MHz,  $\text{CDCl}_3$ )  $\delta$  7.29 (2H, d,  $J=8.8$ ), 6.88 (2H, d,  $J=8.8$ ), 6.15 (1H, s), 5.02 (2H, s), 3.79 (3H, s), 3.26 (2H, s), 3.29 (2H, q,  $J=6.4$ ), 2.32 (2H, t,  $J=8$ ), 1.60 (2H, m), 1.51 (2H, m), 1.24 (32H, s);  $^{13}\text{C}$  NMR (100 MHz,  $\text{CDCl}_3$ )  $\delta$  173.8, 160.6, 159.5, 130.0, 128.1, 113.8, 113.8, 65.9, 55.3, 40.4, 34.3, 29.3, 29.2, 29.1, 29.1, 29.0, 26.7, 25.8, 24.9; HRMS, calcd for  $\text{C}_{22}\text{H}_{32}\text{N}_2\text{O}_4$  ( $\text{M} + \text{Cs}^+$ ) 521.1413, found 521.1429.

**Ester 16**. A solution of 2.0 g of cyano ester **13** (6.3 mmol) and 1.3 g of aldehyde **15** (6.3 mmol) in 20 mL of THF were treated with 0.96 g of DBU (6.3 mmol). The reaction mixture was then warmed to 50 °C and stirred for 12 h. The solvent was removed under reduced pressure and the crude residue was chromatographed (silica, 10–40% ether in hexanes) to yield 2.3 g of compound **16** (4.6 mmol, 76%). **16**: yellow solid; IR (film)  $\nu_{\max}$  3054, 2986, 2305, 2197, 1730, 1666, 1516;  $^1\text{H}$  NMR (400 MHz,  $\text{CDCl}_3$ )  $\delta$  8.00 (1H, s), 7.43 (2H, s), 7.30 (2H, d,  $J=8.8$ ),

6.88 (2H, d,  $J = 8.8$ ), 6.21 (1H, t,  $J = 5.2$ ), 5.04 (2H, s), 3.80 (3H, s), 3.36 (2H, q,  $J = 6.8$ ), 3.31 (4H, t,  $J = 6.0$ ), 2.74 (4H, t,  $J = 7.6$ ), 2.34 (2H, t,  $J = 7.6$ ), 1.95 (4H, m), 1.70–1.54 (4H, m), 1.38 (2H, m);  $^{13}\text{C}$  NMR (100 MHz,  $\text{CDCl}_3$ ) 173.1, 162.2, 159.3, 152.1, 146.8, 130.8, 130.0, 128.0, 120.5, 119.4, 118.4, 113.8, 93.2, 65.9, 55.3, 50.1, 40.1, 34.2, 29.4, 27.6, 26.4, 24.6, 21.2; HRMS, calcd for  $\text{C}_{30}\text{H}_{35}\text{N}_3\text{O}_4$  ( $\text{M} + \text{Cs}^+$ ) 634.1678, found 634.1693.

**Ester 17.** Preparation of this compound was accomplished in 72% yield following the procedure described above for the synthesis of compound **16**. **17**: yellow solid; IR (film)  $\nu_{\text{max}}$  3054, 2986, 2305, 2197, 1730, 1666, 1516;  $^1\text{H}$  NMR (400 MHz,  $\text{CDCl}_3$ )  $\delta$  8.00 (1H, s), 7.42 (2H, s), 7.28 (2H, s), 6.88 (2H, d,  $J = 8.4$ ), 6.22 (1H, s), 5.03 (2H, s), 3.78 (3H, s), 3.37 (2H, q,  $J = 6.8$ ), 3.29 (4H, t,  $J = 5.6$ ), 2.73 (4H, t,  $J = 6.0$ ), 2.39 (2H, t,  $J = 7.2$ ), 1.94 (4H, m), 1.62–1.56 (4H, m), 1.25 (12H, s);  $^{13}\text{C}$  NMR (100 MHz,  $\text{CDCl}_3$ )  $\delta$  173.6, 162.3, 159.4, 152.1, 146.8; 130.8, 129.9, 128.2, 120.6, 119.4, 118.5, 113.8, 113.7, 93.4, 65.7, 55.2, 49.9, 40.27, 34.3, 29.5, 29.31, 29.26, 29.2, 29.1, 29.0, 27.5, 26.8, 24.9, 21.1; HRMS, calcd for  $\text{C}_{35}\text{H}_{45}\text{N}_3\text{O}_4$  ( $\text{M} + \text{H}^+$ ) 572.3487, found 572.3491.

**Acid 18.** 2.2 g of ester **16** (4.4 mmol) were dissolved in 10 mL of a 4:1 mixture of trifluoroacetic acid and anisole and stirred at 25 °C for 10 min. The solvents were initially removed under reduced pressure, and subsequently azeotropically removed using benzene (3  $\times$  10 mL). The residue was then chromatographed (silica, 0–10% methanol in dichloromethane) to produce 1.5 g of carboxylic acid **18** (3.9 mmol, 59%). **18**: red solid; IR (film)  $\nu_{\text{max}}$  2199, 1720, 1647, 1515;  $^1\text{H}$  NMR (400 MHz,  $\text{DMSO}-d_6$ )  $\delta$  7.94 (1H, t,  $J = 5.6$ ), 7.77 (1H, s), 7.40 (2H, s), 3.27 (4H, m), 3.15 (2H, m), 2.66 (4H, m), 2.19 (2H, t,  $J = 7.6$ ), 1.85 (4H, m,  $J = 5.6$ ), 1.48 (4H, m), 1.26 (2H, m);  $^{13}\text{C}$  NMR (100 MHz,  $\text{DMSO}-d_6$ )  $\delta$  174.4, 162.2, 150.0, 146.4, 130.1, 120.3, 118.5, 117.7, 94.9, 49.3, 33.6, 28.8, 27.1, 25.9, 24.2, 20.7; HRMS, calcd for  $\text{C}_{22}\text{H}_{27}\text{N}_3\text{O}_3$  ( $\text{M} + \text{C}^+$ ) 514.1103, found 514.1130.

**Acid 19.** Preparation of this compound was accomplished following the procedure described above for the synthesis of compound **18**. **19**: brown solid; 73%;  $^1\text{H}$  NMR (400 MHz,  $\text{CDCl}_3$ )  $\delta$  8.02 (1H, s), 7.44 (2H, s), 6.27 (1H, t,  $J = 5.6$ ), 3.45 (4H, m), 3.29 (2H, m), 2.83 (4H, t,  $J = 6.4$ ), 2.43 (2H, t,  $J = 7.6$ ) 2.04 (4H, t,  $J = 6$ ), 1.64–1.53 (4H, m), 1.28 (12H, s);  $^{13}\text{C}$  NMR (100 MHz,  $\text{CDCl}_3$ )  $\delta$  179.0, 162.5, 152.3, 146.9, 130.9, 120.6, 119.5, 118.5, 93.2, 50.0, 40.3, 33.9, 29.5, 29.2, 29.3, 29.1, 29.1, 28.9, 27.6, 26.8, 24.6, 21.2; HRMS, calcd for  $\text{C}_{27}\text{H}_{37}\text{N}_3\text{O}_3$  ( $\text{M} + \text{Cs}^+$ ) 584.1886, found 584.1899.

**Phospholipid 22.** To a solution of 138 mg of acid **18** (0.33 mmol) in 3 mL of chloroform were added 107 mg of lysophospholipid **20** (0.33 mmol), 64 mg of EDC (0.33 mmol), and 40 mg of DMAP (0.33 mmol) and the reaction was stirred for 18 h at 25 °C. The solvent was removed under reduced pressure and the resulting residue was purified by reversed phase flash chromatography (0–100% acetonitrile/water) to give 157 mg of phospholipid **22** (54%). **22**: red liquid; IR (film)  $\nu_{\text{max}}$  3377, 2924, 2852, 2200, 1735, 1664;  $^1\text{H}$  NMR (400 MHz,

$\text{CDCl}_3$ )  $\delta$  7.97 (1H, s), 7.42 (2H, s), 6.44 (1H, t,  $J = 5.6$ ), 5.21–5.19 (1H, m), 4.38–4.23 (3H, m), 4.15–4.10 (1H, m), 3.98 (2H, t,  $J = 6.4$ ), 3.83 (2H, s), 3.38 (11H, s), 3.29 (4H, t,  $J = 5.6$ ), 2.73 (4H, t,  $J = 6.4$ ), 2.34–2.25 (4H, m), 1.97–1.91 (4H, m), 1.65–1.52 (4H, m), 1.4–1.35 (2H, m), 1.23 (16H, s), 0.86 (3H, t,  $J = 6.8$ );  $^{13}\text{C}$  NMR (100 MHz,  $\text{CDCl}_3$ )  $\delta$  173.3, 172.7, 162.3, 152.9, 146.8, 130.8, 120.5, 119.3, 118.4, 93.4, 70.6, 70.4, 66.3, 63.5, 62.9, 59.3, 54.5, 50.1, 40.1, 34.1, 32.0, 29.7, 29.7, 29.6, 29.4, 29.4, 29.3, 29.2, 27.7, 26.4, 26.3, 24.9, 24.6, 22.7, 21.3, 14.2; HRMS  $m/z$  calcd for  $\text{C}_{42}\text{H}_{67}\text{N}_4\text{O}_9\text{P}$  ( $\text{M} + \text{H}^+$ ) 803.4718, found 803.4682.

**Phospholipid 23.** Preparation of this compound was accomplished following the procedure described above for the synthesis of compound **22**. **23**: IR (film)  $\nu_{\text{max}}$  3377, 2924, 2852, 2200, 1735, 1664;  $^1\text{H}$  NMR (400 MHz,  $\text{CDCl}_3$ )  $\delta$  7.95 (1H, s), 7.42 (2H, s), 6.44 (1H, t,  $J = 5.6$ ), 5.20–5.17 (1H, m), 4.38–4.34 (3H, m), 4.15–4.10 (1H, m), 3.98 (2H, t,  $J = 6.4$ ), 3.84 (2H, s), 3.38 (11H, s), 3.29 (4H, t,  $J = 5.6$ ), 2.73 (4H, t,  $J = 6.4$ ), 2.34–2.25 (4H, m), 1.97–1.91 (4H, m), 1.65–1.52 (4H, m), 1.4–1.35 (2H, m), 1.23 (26H, s), 0.86 (3H, t,  $J = 6.8$ );  $^{13}\text{C}$  NMR (100 MHz,  $\text{CDCl}_3$ )  $\delta$  173.3, 172.7, 162.3, 152.9, 146.8, 130.8, 120.5, 119.3, 118.2, 93.4, 70.6, 70.5, 66.3, 63.6, 62.8, 59.4, 54.4, 50.1, 40.1, 34.1, 32.0, 29.7, 29.6, 29.4, 29.3, 29.2, 27.6, 26.3, 24.9, 24.6, 22.7, 21.2, 14.2; HRMS  $m/z$  calcd for  $\text{C}_{46}\text{H}_{75}\text{N}_4\text{O}_9\text{P}$  ( $\text{M} + \text{H}^+$ ) 859.3544, found 859.5322.

**Phospholipid 24.** Preparation of this compound was accomplished in 48% yield following the procedure described above for the synthesis of compound **22**. **24**: red solid;  $^1\text{H}$  NMR (400 MHz,  $\text{CDCl}_3$ )  $\delta$  7.98 (1H, s), 7.41 (2H, s), 6.22 (1H, t,  $J = 5.2$ ), 5.17 (1H, m), 4.38–4.28 (3H, m), 4.12–4.08 (1H, m), 3.93 (2H, d,  $J = 6.0$ ), 3.78 (2H, s), 3.37 (11H, s), 4.29 (4H, t,  $J = 5.2$ ), 2.72 (4H, t,  $J = 6.0$ ), 2.28–2.23 (5H, m), 1.96–1.90 (4H, m), 1.55 (7H, s), 1.23 (40H, s), 0.85 (3H, t,  $J = 6.4$ );  $^{13}\text{C}$  NMR (100 MHz,  $\text{CDCl}_3$ )  $\delta$  173.4, 173.1, 162.0, 152.1, 146.87, 130.9, 120.6, 119.4, 118.6, 93.5, 70.5, 70.4, 66.3, 63.3, 62.9, 59.2, 54.4, 50.0, 40.3, 34.3, 34.1, 31.9, 29.7, 29.6, 29.6, 29.5, 29.4, 29.4, 29.3, 29.3, 29.2, 29.1, 29.1, 27.6, 26.9, 24.9, 24.8, 22.6, 21.2, 14.1; HRMS  $m/z$  calcd for  $\text{C}_{51}\text{H}_{85}\text{N}_4\text{O}_9\text{P}$  ( $\text{M} + \text{H}^+$ ) 929.4327, found 929.4339.

**Compound 28.** To a solution of 51 mg cyano acetic *p*-nitro phenolate (0.25 mmol) in 0.5 mL  $\text{CDCl}_3$ , was added 160 mg (0.25 mmol) dimyristoyl-L- $\alpha$ -phosphatidyl ethanolamine (C14:0) and 31 mg (0.25 mmol) DMAP and the reaction was stirred at 25 °C for 12 h. The solvent was then removed under reduced pressure and the residue was dissolved in THF (1.5 mL) and treated with 42 mg of DBU (0.25 mmol) and 52 mg of aldehyde **15** (0.28 mmol). The reaction mixture was stirred at 50 °C for 12 h. The solvent was removed under reduced pressure and the residue was purified on silica (0–8% methanol in dichloromethane) to yield 85 mg of phospholipid **28** (38%). **28**: bright yellow liquid; IR (film)  $\nu_{\text{max}}$  3370, 2923, 2852, 2201, 1738, 1516;  $^1\text{H}$  NMR (400 MHz,  $\text{CD}_3\text{OD}$ )  $\delta$  7.76 (1H, s), 7.34 (2H, s), 5.10 (1H, m), 4.38–4.28 (1H, m), 4.10–4.02 (1H, m), 3.90–3.79 (3H, m), 3.21–3.09 (4H, m), 2.63–2.56 (4H, m), 1.91 (2H, m,  $J = 5.6$ ), 1.84 (2H, m,  $J = 6.0$ ), 1.70–1.41 (12H,

m), 1.15 (40H, s), 0.78 (6H, t,  $J=5.2$ );  $^{13}\text{C}$  NMR (100 MHz,  $\text{CDCl}_3$ )  $\delta$  172.5, 172.3, 165.5, 150.7, 146.4, 130.2, 120.22, 118.3, 117.9, 71.4, 71.4, 65.6, 65.1, 63.7, 55.6, 51.3, 49.7, 48.3, 37.6, 33.9, 33.7, 31.7, 31.6, 29.4, 29.3, 29.2, 29.1, 28.9, 28.7, 27.3, 26.5, 24.6, 23.7, 22.4, 20.9, 19.2, 13.3; HRMS  $m/z$  calcd for  $\text{C}_{49}\text{H}_{80}\text{N}_3\text{O}_9\text{P}$  ( $\text{M}-\text{H}^+$ ) 884.5559, found 884.5518.

### Determination of physical properties

Stock solutions of **22**, **23**, **24**, **28**, and **1** were prepared at a concentration of 10 mM in chloroform. For the determination of the relationship between quantum yield and viscosity of the medium, mixtures of ethylene glycol and glycerol were prepared. Different viscosities were achieved by different volume/volume mixture ratios of ethylene glycol/glycerol as follows: 7:3 (49 cP), 5:5 (115 cP), 4:6 (163 cP), 3:7 (245 cP), 2:8 (391 cP) following an experiment described previously.<sup>12,21</sup> 3.5 mL of each of these mixtures was placed into a spectroscopic cuvette. Then, 10  $\mu\text{L}$  of probe stock solution was added. The emission intensity of each of the five samples was acquired using a Spex FluoroMax 3 fluorophotometer (Jobin-Yvon, Edison, NJ, USA). Excitation wavelength was set to 470 nm and an emission scan performed from 480 to 550 nm. The maximum was recorded and plotted against the viscosity in double-logarithmic scale. A straight line was fitted to the logarithmized data points using the least-squares method, and the slope obtained.

### Preparation and measurement of stained liposomes

Dimyristoylphosphatidylcholine (DMPC), dissolved in chloroform at 25 mg/mL, was purchased from Avanti Polar Lipids. To 400  $\mu\text{L}$  of this solution was added 20  $\mu\text{L}$  of the 10 mM probe stock solution. In a glass vial, the chloroform was evaporated under nitrogen at 0 °C. 8 mL phosphate-buffered saline (PBS, Irvine Scientific) was added. After sonication, liposomes were created by extruding the mixture through a 400-nm filter at 37 °C. The final liposome suspension was placed into a spectroscopic glass cuvette and placed in a Shimadzu RF-1501 spectrophotometer (Shimadzu, Kyoto, Japan) equipped with a temperature-controlled cuvette holder and a time-based acquisition program. The liposome suspension was cooled to 10 °C in the fluorospectrometer. At fixed wavelengths  $\lambda_{\text{ex}}=470$  nm and  $\lambda_{\text{em}}=490$  nm, emission intensity was recorded while the temperature was raised from 10 to 40 °C over a period of 5 min. Temperature and intensity were recorded simultaneously.

### Preparation and microscopy of stained cells

Immortalized endothelial cells of the cell line ECV-304 (ATCC) were seeded onto glass coverslips at a density of 800,000  $\text{mL}^{-1}$  and grown to confluence in M199, supplemented with 10% fetal calf serum (FCS) within 24 h. The dyes, **22**, **23**, **24**, and **28**, were delivered to the cells in the form of micelles as follows:<sup>22</sup> Micelles were prepared by dissolving 0.25 mg sodium deoxycholate (Sigma, St Louis, MO, USA) in 5 mL of a mixture of

$\text{CHCl}_3$  and methanol (2:1), then adding 100  $\mu\text{L}$  of the probe stock solution (10 mM in  $\text{CHCl}_3$ ). The fluid was dried under nitrogen on ice, then resuspended in 10 mL phosphate-buffered saline (PBS) and sonicated for 10 min.

Staining solution for DiI-C<sub>18</sub> was prepared by adding 5  $\mu\text{L}$  Vybrant DiI labeling solution (Molecular Probes, Eugene, OR, USA) to 1 mL PBS. Cell staining was performed by washing the slides in PBS, then covering the slide surface with 1 mL of the DiI staining medium. After 20 min incubation in the dark at 37 °C, the slides were washed in PBS and the micelle suspension was added in a similar manner with an incubation time of 10 min. After the incubation period, the slides were washed again and immediately examined under the microscope (Nikon Diaphot TMD with DVC-1310 CCD camera acquisition system). Fluorescent images were obtained by acquiring one image with the G1B filter set (dyes **22**, **23**, **24**, and **28**) and a second image by switching to the Texas Red filter set without moving the sample. The two images were merged using the red channel for DiI and the green channel for **22**, **23**, **24**, and **28**.

### Acknowledgements

This research was partially supported by the NIH (HL-40696 and CA-85600).

### References and Notes

1. For Selected Accounts On Cell Membrane-Related Topics, see: Morre, D. J., Howell, K. E., Bergeron, J. J. M., Eds. *Molecular Mechanisms of Membrane Traffic*. Springer: New York, 1993. Rohrbach, D. H., Timpl, R., Eds. *Molecular and Cellular Aspects of Basement Membranes*. Academic: San Diego, 1993. Yeagle, P. L., Ed. *The Membranes of Cells*. Academic: San Diego, 1993. Haber, E., Ed. *The Cell Membrane: Its Role in Interaction with the Outside World*. Plenum: New York, 1984.
2. (a) Singer, S. J.; Nicolson, G. L. *Science* **1972**, *175*, 720. (b) Singer, S. J. *Ann. Rev. Biochem.* **1974**, *43*, 805.
3. Lakowicz, J. R. Ed. *Principles of Fluorescence Spectroscopy*. Kluwer Academic/Plenum: New York, 1999 (2nd ed.).
4. Axelrod, D.; Koppel, D. E.; Schlessinger, J.; Elson, E.; Webb, W. W. *Biophys. J.* **1976**, *16*, 1055. Swaminathan, R.; Bicknese, S.; Periasamy, N.; Verkman, A. S. *Biophys. J.* **1996**, *71*, 1140.
5. Shinitzky, M.; Barenholz, Y. *Biochim. Biophys. Acta* **1978**, *515*, 367.
6. Parasassi, T.; Di Stefano, M.; Loiero, M.; Ravagnan, G.; Gratton, E. *Biophys. J.* **1994**, *66*, 763. Rettig, W., Lapouyade, R. Fluorescence Probes Based on Twisted Intramolecular Charge Transfer (TICT) States and Other Adiabatic Photo-reactions. In *Topics in Fluorescence Spectroscopy, Vol. 4, Probe Design and Chemical Sensing*: Lakowicz, J. R., Ed.; Plenum: New York, 1994; p 109.
7. Loutfy, R. O. *Pure Appl. Chem.* **1986**, *58*, 1239. Williams, M. L.; Landel, R. F.; Ferry, J. D. *J. Am. Chem. Soc.* **1955**, *84*, 2803. Kasatai, K.; Kawasaki, M.; Sato, H. *Chem. Phys.* **1984**, *83*, 461. Iwaki, T.; Torigoe, C.; Noji, M.; Nakanishi, M. *Biochemistry* **1993**, *32*, 7589. Haidekker, M. A.; L'Heureux, N.; Frangos, J. A. *Am. J. Physiol. Heart Circ. Physiol.* **2000**, *278*, H1401.

8. Viriot, M. L.; Carre, M. C.; Geoffroy-Chapotot, C.; Brembilla, A.; Muller, S.; Stoltz, J.-F. *Clin Hemorheol. Microcirc.* **1998**, *19*, 151.
9. Kung, C. E.; Reed, J. K. *Biochemistry* **1989**, *28*, 6678.  
Sawada, S.; Iio, T.; Hayashi, Y.; Takahashi, S. *Anal. Biochem.* **1992**, *204*, 110. Iio, T.; Takahashi, S.; Sawada, S. *J. Biochem.* **1993**, *113*, 196.
10. Haidekker, M. A.; Ling, T.; Anglo, M.; Stevens, H. Y.; Frangos, J. A.; Theodorakis, E. A. *Chem. Biol.* **2001**, *8*, 123.
11. Yokokawa, F.; Toshinobu, A.; Takayuki, S. *Org. Lett.* **2000**, *2*, 4169.
12. Sigeru, T.; Hideo, T.; Masatoshi, T.; Yutaka, K.; Michio, S.; Takashi, S.; Ryo, K.; Ichiro, K.; Akihiro, S.; Shigemitsu, N. *J. Org. Chem.* **1991**, *56*, 3633.
13. Förster, Th.; Hoffmann, G. *Z. Phys. Chem.* **1971**, *75*, 63.
14. Lukac, S. *J. Am. Chem. Soc.* **1984**, *106*, 4386.
15. Honig, M. G.; Hume, R. I. *Cell Biol.* **1986**, *103*, 171. Wolf, D. E.; Scott, B. K.; Millette, C. F. *J. Cell Biol.* **1986**, *103*, 1745.  
Ledley, F. D.; Soriano, H. E.; O'Malley, B. W., Jr.; Lewis, D.; Darligto, G. J.; Finegold, M. *Biotechniques* **1992**, *580*, 584.  
Axelrod, D. *Biophys. J.* **1979**, *26*, 557.
16. Edidin, M. Fluorescence Photobleaching and Recovery, FPR, in the Analysis of Membrane Structure and Dynamics. In *Mobility and Proximity in Biological Membranes*; Damjanovich, S., Edidin, M., Eds.; CRC: Boca Raton, 1994 p 109.
17. Abdul-Rahim, H.; Bouchy, M. *J. Photochem. Photobio. B: Biol.* **1998**, *47*, 95.
18. (a) van Ginkel, G.; van Langen, H.; Levine, Y. K. *Biochimie* **1989**, *71*, 23. (b) Mulders, F.; van Langen, H.; van Ginkel, G.; Levine, Y. K. *Biochim. Biophys. Acta* **1986**, *859*, 209. Chapman, D. Biomembrane Fluidity: The Concept and Its Development; In *Membrane Fluidity in Biology*; Aloia, R. C., Ed.; Academic: New York, London, 1983; p 5.
19. Loufty, R. O.; Law, K. Y. *J. Phys. Chem.* **1980**, *84*, 2803. Sundström, V.; Gillbro, T. *J. Phys. Chem.* **1982**, *86*, 1788.
20. Dimova, R.; Pouligny, B.; Dietrich, C. *Biophys. J.* **2000**, *79*, 340.
21. Iwaki, T.; Torigoe, C.; Noji, M.; Nakanishi, M. *Biochemistry* **1993**, *32*, 7589.
22. Began, G.; Sudharsan, E.; Appu Rao, A. G. *Biochemistry* **1999**, *38*, 13920.